International Journal of Non-Linear Mechanics 46 (2011) 321–329

Contents lists available at ScienceDirect

International Journal of Non-Linear Mechanics

journal homepage: www.elsevier.com/locate/nlm

Hysteretic deteriorating model for quasi-brittle materials based on micromechanical damage approach

Xiaodan Ren, Jie Li *

School of Civil Engineering, Tongji University, 1239 Siping Road, Shanghai 200092, China

ARTICLE INFO

Article history:
Received 4 January 2010
Received in revised form
2 August 2010
Accepted 21 September 2010

Keywords:
Micromechanical damage model
Deterioration
Hysteresis
Parallel element model
Quasi-brittle materials

ABSTRACT

A damage model, which is based on the stochastic modeling of the microstructures, is developed for the quasi-brittle materials subjected to repeated loading. According to this model, the overall response of the material is represented with a series of micro-elements joined in parallel. A combined model is proposed for the micro-element considering the fracture as well as the hysteretic energy dissipation. To account for the progressive failure, the random fracture strains are assigned to the micro-elements. Therefore the overall parallel bundle is considered as a stationary random field. Then by averaging the microscopic random field, the overall loading, unloading and reloading curves are derived analytically. Two hysteretic rules are derived from the proposed model, and the overall hysteretic deteriorating behaviors could be well reproduced. To demonstrate the validity of the present model, the numerical results are shown against the stochastic simulated curves as well as the experimental data. The present model provides an alternative approach for the efficient modeling of the hysteretic deteriorating behaviors for the quasi-brittle materials.

1. Introduction

The mechanical modeling of the quasi-brittle materials such as concrete and rock is one of the essential topics in the research of the civil engineering. However, the physical modeling of concrete as well as rock is still quite challenging due to their inherent complexity. It is observed from the experiments that the failure of the quasi-brittle solids is commonly characterized by the nucleation and propagation of micro-cracks subjected to tensile and shear tractions, and often involves contact and friction on these surfaces under certain loading conditions. The propagation of the micro-cracks is often represented as the deterioration and descending of the load–displacement curve. And the friction on the cracked surfaces leads to the plastic deformations. Hence a considerable number of studies are stressed to develop the theoretical models for the simulation of such phenomenon. Among these researches, the continuum damage model was intensively investigated in recent years. Several celebrated works, e.g. [1–3] and so on, were proposed to consider the multi-dimensional damage behaviors for concrete on the basis of thermal dynamics and have been widely adopted for structural non-linear analysis. However, the development of the damage evolution function seems to be controversial within continuum mechanics framework. The irreversible thermal dynamics merely regulates the reasonable range of the non-linear evolutions rather than specifies their expressions. Hence most continuum damage models just directly adopt the damage evolution expressions identified by the experimental data with many empirical material parameters. In the present paper, we investigate the uniaxial behaviors of quasi-brittle materials under non-uniform repeated loading by idealized micromechanical model and express the non-linear evolutions in terms of damage variable. This work provides an alternative approach to develop the damage evolution functions for continuum damage mechanics.

According to the uniaxial idealized micromechanical model, structural element can be idealized as a sequence of micro-elements jointed in a system. The individual elements represent the microscopic properties of the material. And the system represents the macro or structural response. The bridge between the two scales is the probability distribution which describes the mechanical properties of the micro-elements. Therefore, complex macro-material behaviors can be developed based on the parallel system in which individual elements are endowed with simple material properties. Two classes of micromechanical models are often adopted for the material modeling, e.g. the serial element model and the parallel element model. The former one is also known as the Preisach model, which was proposed by the German physicist Preisach [4]. Later, Krasnoselskii [5] developed the mathematical structure for this model. In recent 20 years, this model was intensively investigated and applied to the modeling of hysteresis for piezoelectric materials ([6–8], and so on). The other class of models was proposed mainly for the modeling of

* Corresponding author. Tel.: +86 02165983526; fax: +86 02165983944.
E-mail address: lijie@tongji.edu.cn (J. Li).

0020-7462/$ - see front matter © 2010 Elsevier Ltd. All rights reserved.
doi:10.1016/j.ijnonlinmec.2010.09.015

material hysteresis and failure under uniaxial loading. And the proposed model is developed based on the parallel element models (Fig. 1).

Historically, the parallel element model was firstly proposed to estimate the rupture strength of fibrous materials such as threads, cables and woods [9,10]. Later, this simple but elaborate model was extensively applied to the simulations of brittle [11–13] and ductile [14–18] phenomenon. Eibl and Schmidt-Hurtienne [19] and Valipour et al. [20] proposed the rate dependent model for concrete beams based on the parallel elements model. Bazant and Pang [21] also investigated the size effect of concrete on the basis of the parallel elements model.

The simplest model to describe the progressive damage propagation for a brittle bar subjected to uniaxial loading was provided by a loose bundle parallel bar system. According to this model, each element is endowed with common stiffness but different rupture strength. And the random distribution of the rupture strength is given. Then the monotonic load–displacement behavior of the brittle materials is obtained by averaging the stochastic microstructures (Fig. 2). It is observed that the failure strength as well as the load–displacement curve is deterministic in the limiting case when the numbers of elements approaching infinity due to the independence among each element. By noting this, an extended model was proposed by Kandarpa et al. [32] to represent the randomness of the load–displacement responses for the brittle materials. In this model, the failure stresses of the micro-elements are considered as a random field. With proper consideration of the distribution and the spatial correlation, the statistics including the mean value and the standard derivation of the load–displacement curves are analytically derived for the parallel system. In Li and Zhang [22], the fracture strains of the micro-elements were defined as random field thus a uniaxial stochastic damage model was developed for concrete.

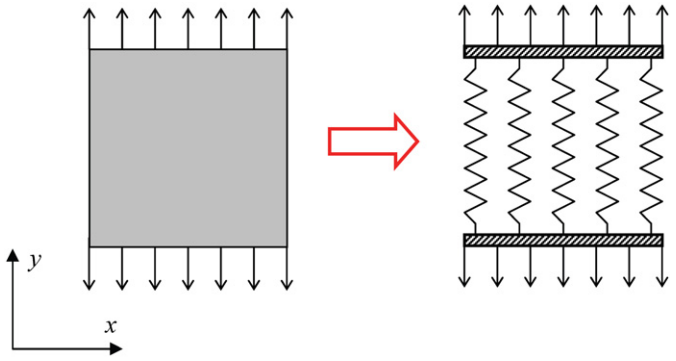

Fig. 1. Parallel element model.

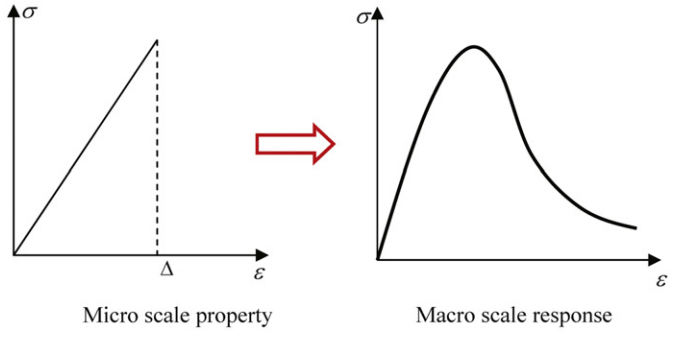

Fig. 2. Brittle behaviors in two scales.

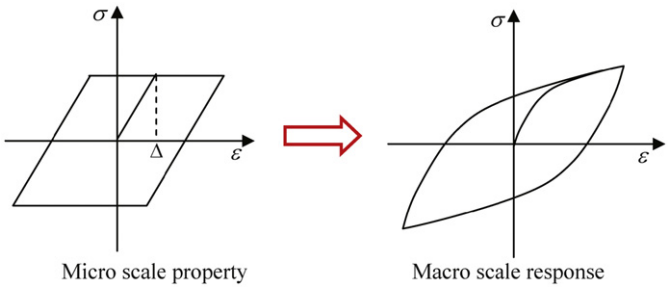

Fig. 3. Ductile behaviors in two scales.

On the other hand, the parallel element model for ductile materials is often developed for the modeling of the hysteretic behaviors. In fact, as early as 1926, Masing proposed a series of phenomenological rules to elucidate how to establish hysteretic loop according to monotonic loading curve for ductile materials [23]. In the middle of 1960s, Iwan introduced such a parallel-series model (DEM) for hysteretic systems [14]. This model consists of a series of ideal elasto-plastic elements connected in parallel with a common stiffness but different yield strengths. If the distribution of yield strengths is known, the stress–strain curves for ductile materials under cyclic loading is obtained based on either stochastic simulation or averaging methods (Fig. 3). It is interesting that the Iwan model shows the Masing-type behavior [15]. Later by assigning the rupture threshold after yield for the elasto-plastic elements, Iwan represented deterioration with his model [24]. Recently, Ashrafi and Andrew [25], Ashrafi and Smyth [26] proposed the equivalent generalized Masing rule in order to determine the deteriorating behaviors.

Unfortunately, neither the brittle type nor the ductile type parallel element model provides excellent simulating results for the quasi-brittle materials subjected to repeated loading due to the inherent coupling of damage and plasticity. Therefore, the aim of this paper is to develop a micromechanical damage model which can account for both the softening and the hysteretic behaviors for the quasi-brittle materials. This paper is structured as follows: a idealized stress–strain model is first proposed to describe the behaviors of micro-elements. The fracture strains of the micro-elements are considered as random field. Then the loading, unloading and reloading curves are analytical derived based on the stochastic averaging approach. Several simulating results are presented against experimental data, whose results allow for demonstrating its capacity of reproducing the salient features for the quasi-brittle materials subjected to repeated loading.

2. Problem formulation

2.1. Micro-element model

As mentioned above, the elastic-perfectly fracture model and the elastic-perfectly plastic model (Figs. 2 and 3) were adopted to describe the elastic damage and the ductile hysteretic behaviors correspondingly. However, most of the deformation processes for the real materials are neither perfectly brittle nor purely ductile. For the quasi-brittle materials, both the damage and progressive failure play important part throughout the entire deformation process; meanwhile, the plastic deformation rectifies the unloading and reloading behaviors. Actually, the typical deformation process for the quasi-brittle materials could be divided into two stages. Before rupture, the linear elastic behaviors could be observed. There is a sudden stress drop when the fracture strain is

achieved. Then the residual stress is determined due to the cohesive stress and the friction between the cracking surfaces.

Therefore, the fracture-ductile material model is proposed for micro-element modeling of the quasi-brittle material (Fig. 4). Four elements are adopted to assemble the combined micro-element model. The main elastic element represents the elastic deformation of the material matrix; the fracture element defines the fracture stress σ_c of the specimen; the friction element describes the residual stress σ_s for the material; and the secondary elastic element identifies the elastic behaviors of the cracked specimen.

By observing the fracture-ductile micro-element and using the Heaviside function, the loading stress–strain relationship is expressed as

$$\sigma = H(\Delta-\varepsilon)E\varepsilon + H(\varepsilon-\Delta)\sigma_s \tag{1}$$

where $H(\bullet)$ is the Heaviside function, E is the elastic modulus, Δ is the fracture strain and σ_s is the residual stress. According to the testing results of Ye [27] and Tao [28], the residual stress σ_s can be defined as linear function of the fracture stress σ_c as follows:

$$\sigma_s = \eta_s\sigma_c = \eta_s E\Delta \tag{2}$$

where η_s is the shear retention coefficient. Substituting Eq. (2) into Eq. (1), one obtains

$$\sigma = [1-H(\varepsilon-\Delta)]E\varepsilon + \eta_s E\Delta H(\varepsilon-\Delta) \tag{3}$$

The monotonic loading stress–strain curve is shown in Fig. 5.

In unloading and reloading stages, the uncracked element remains elastic (Fig. 4). And the hysteretic behavior of the cracked element should be carefully considered. Based on the micro-element configurations after rupture shown in Fig. 4, a bi-linear hysteresis behavior could be obtained. The unloading and the reloading behaviors of the micro-elements are shown in Fig. 6. The unloading and reloading stiffness of the cracked element is

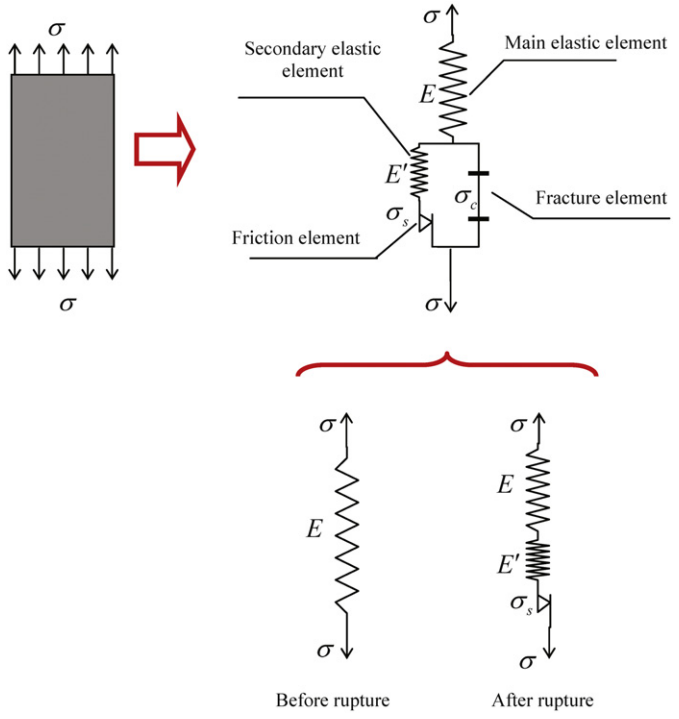

Fig. 4. The fracture-ductile micro-element.

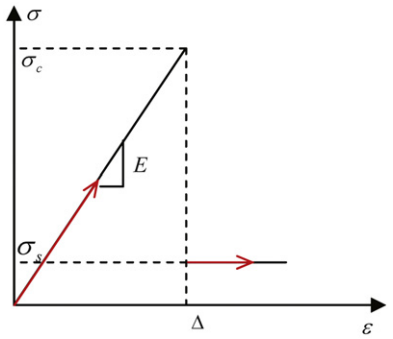

Fig. 5. Loading stress—strain curve for the micro-element.

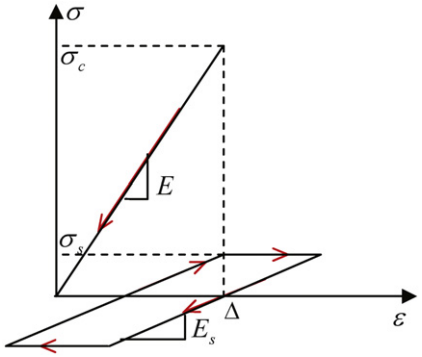

Fig. 6. Unloading and reloading behaviors for the micro-element.

derived as follows:

$$E_s = \frac{E'}{E'+E}E \triangleq \eta_e E \tag{4}$$

where η_e is defined as the stiffness decreasing coefficient.

Let $(\varepsilon_{\max}, \sigma_{\max})$ be the unloading point on the monotonic loading curve, the stress–strain relationship could be expressed using the piecewise function as follows:

$$\sigma_{\max}-\sigma = \begin{cases} E_0(\varepsilon_{\max}-\varepsilon) & \text{if} \quad \Delta-\varepsilon_{\max} > 0 \\ \eta_e E_0(\varepsilon_{\max}-\varepsilon) & \text{if} \quad \Delta-\varepsilon_{\max} \le 0 \text{ and } \varepsilon_{\max}-\varepsilon < \dfrac{2\eta_s}{\eta_e}\Delta \\ 2\eta_s E_0\Delta & \text{if} \quad \Delta-\varepsilon_{\max} \le 0 \text{ and } \varepsilon_{\max}-\varepsilon \ge \dfrac{2\eta_s}{\eta_e}\Delta \end{cases} \tag{5}$$

Using the Heaviside function, Eq. (5) is rewritten as

$$\sigma_{\max}-\sigma = \phi_1(\varepsilon_{\max}-\varepsilon) + \phi_2(\varepsilon_{\max}-\varepsilon) + \phi_3(\varepsilon_{\max}-\varepsilon) \tag{6}$$

where

$$\phi_1 = H(\Delta-\varepsilon_{\max})E(\varepsilon_{\max}-\varepsilon) \tag{7}$$

$$\phi_2 = H(\varepsilon_{\max}-\Delta)H\left[\frac{2\eta_s}{\eta_e}\Delta-(\varepsilon_{\max}-\varepsilon)\right]\eta_e E(\varepsilon_{\max}-\varepsilon) \tag{8}$$

$$\phi_3 = H(\varepsilon_{\max}-\Delta)H\left[(\varepsilon_{\max}-\varepsilon)-\frac{2\eta_s}{\eta_e}\Delta\right]2\eta_s E\Delta \tag{9}$$

It is observed from Fig. 6 that both the loading straight line and the hysteretic loop are rotational symmetric. Hence the reloading function could be obtained from Eq. (6) through the rotational transformation. Let $(\varepsilon_{\min}, \sigma_{\min})$ be the reloading point on the

unloading curve. Then replace the terms $(\varepsilon_{\max}, -\varepsilon)$ and $(\sigma_{\max} - \sigma)$ in Eq. (6) with $(\varepsilon, \varepsilon_{\min})$ and $(\sigma, \sigma_{\min})$ correspondingly, one gets the reloading function as follows:

$$\sigma - \sigma_{\min} = \phi_1(\varepsilon - \varepsilon_{\min}) + \phi_2(\varepsilon - \varepsilon_{\min}) + \phi_3(\varepsilon - \varepsilon_{\min}) \tag{10}$$

If the current strain ε exceeds the original unloading strain $\varepsilon_{\max}$, the stress–strain path will return to the monotonic loading curve expressed by Eq. (3).

2.2. Macro-system formulation

Consider the parallel element system illustrated in Fig. 1. In the present paper, the micro-elements are endowed with common stiffness but different fracture stresses. Moreover, the identical stiffness decreasing coefficient is adopted for each element so that each of them is endowed with common unloading and reloading stiffness. Suppose the fracture strain $\Delta(x)$ is a stationary random field with the first-order density functions as follows:

$$f(\Delta; x) = f(\Delta) \tag{11}$$

where x is the spatial coordinate of the random field. Then the first-order cumulative distribution function of $\Delta(x)$ is

$$F(\varepsilon) = \int_{-\infty}^{\varepsilon} f(\Delta)\, d\Delta \tag{12}$$

And define the first-order moment function as follows:

$$G(\varepsilon) = \int_{-\infty}^{\varepsilon} \Delta f(\Delta)\, d\Delta \tag{13}$$

It is clearly that $F(\varepsilon)$ and $G(\varepsilon)$ could be numerically calculated by using $f(\Delta)$.

Let σ_i be the stress of the ith element in the bundle, one obtains

$$\sigma_i = \sigma(x_i), \quad i = 1,2\ldots M \tag{14}$$

where x_i denotes the spatial coordinate of the ith element and M is the total number of the elements in the parallel system. Assume that all the elements are endowed with the same sectional area. Then the stress of the parallel system is

$$\overline{\sigma} = \frac{1}{M}\sum_{i=1}^{M} \sigma(x_i) \tag{15}$$

Performing a limit of Eq. (15) as M approaches infinity and accounting for the definition of the stochastic integration, we get

$$\overline{\sigma} = \int_0^1 \sigma(x)\, dx \tag{16}$$

Eq. (16) represents the relationship between micro-stress and macro-stress.

The micro-elements in the bundle could be classified into two categories: cracked part and uncracked part (Fig. 7). Hence, the split of the macro-stress was introduced as follows:

$$\overline{\sigma} = \overline{\sigma}^d + \overline{\sigma}^s \tag{17}$$

where $\overline{\sigma}^d$ is the overall stress of the uncracked bundle, and $\overline{\sigma}^s$ is the overall stress of the cracked bundle. According to Eq. (15), $\overline{\sigma}^d$ could be expressed as

$$\overline{\sigma}^d = \frac{1}{M}\sum_{i=1}^{M} H(\Delta_i - \varepsilon)\sigma(x_i) \tag{18}$$

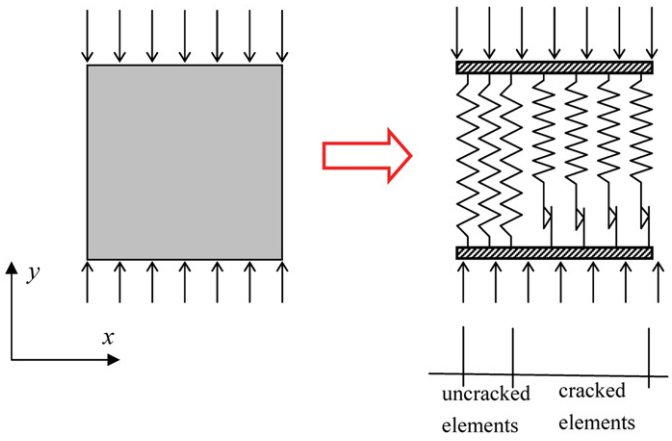

Fig. 7. Parallel element model.

where Δ_i denotes the rupture strain of the micro-element located in x_i. Due to the elasticity of the uncracked elements, one obtains

$$\overline{\sigma}^d = \left[\frac{1}{M}\sum_{i=1}^{M} H(\Delta_i - \varepsilon)\right] E\varepsilon = \left[1 - \frac{1}{M}\sum_{i=1}^{M} H(\varepsilon - \Delta_i)\right] E\varepsilon \tag{19}$$

Performing a limit of Eq. (19) as M approaches infinity we obtain

$$\overline{\sigma}^d = \left\{1 - \int_0^1 H[\varepsilon - \Delta(x)]\, dx\right\} E\varepsilon \tag{20}$$

On the other hand, the classic definition of damage gives

$$d = \frac{A_d}{A} \tag{21}$$

where A_d and A are the cracked area and the initial undamaged area, respectively. Accounting for Eq. (21) and using the Heaviside function, the damage index for the parallel element model is defined as

$$d(\varepsilon) = \frac{1}{M}\sum_{i=1}^{M} H(\varepsilon - \Delta_i) \tag{22}$$

Again, performing a limit of Eq. (22) as M approaches infinity and accounting for the definition of the stochastic integration, one obtains

$$d(\varepsilon) = \int_0^1 H[\varepsilon - \Delta(x)]\, dx \tag{23}$$

Substitute Eq. (23) into Eq. (20), we obtain

$$\overline{\sigma}^d = [1 - d(\varepsilon)]E\varepsilon = [1 - d(\varepsilon)]\overline{\sigma}^e \tag{24}$$

where $\overline{\sigma}^e$ is the elastic effective stress.

$\overline{\sigma}^s$ represents the overall remnant stress of the bundle. By analogy with Eq. (18), $\overline{\sigma}^s$ could be expressed as follows:

$$\overline{\sigma}^s = \frac{1}{M}\sum_{i=1}^{M} H(\varepsilon - \Delta_i)\sigma(x_i) \tag{25}$$

Performing a limit of Eq. (25), we obtain

$$\overline{\sigma}^s = \int_0^1 H[\varepsilon - \Delta(x)]\sigma(x)\, dx \tag{26}$$

The analytical expressions of $\overline{\sigma}^d$ and $\overline{\sigma}^s$ will be discussed in the following part considering the hysteretic loading condition.

2.2.1. Monotonic loading curve

Substituting Eq. (3) into Eq. (16), we obtain the monotonic loading curve for the parallel system as follows:

$$\overline{\sigma}=\left\{1-\int_0^1 H[\varepsilon-\Delta(x)]dx\right\}E\varepsilon+\eta_s E\int_0^1 \Delta(x)H[\varepsilon-\Delta(x)]dx \tag{27}$$

Comparing Eq. (27) with Eq. (17), and considering Eqs. (24) and (26), we obtain

$$\overline{\sigma}^d=\left\{1-\int_0^1 H[\varepsilon-\Delta(x)]dx\right\}E\varepsilon=[1-d(\varepsilon)]E\varepsilon \tag{28}$$

$$\overline{\sigma}^s=\eta_s E\int_0^1 \Delta(x)H[\varepsilon-\Delta(x)]dx \tag{29}$$

Let $\mu(\bullet)$ be the expectation operator. Then performing the expectation operator to Eq. (28), we get

$$\mu[\overline{\sigma}^d]=\{1-\mu[d(\varepsilon)]\}E\varepsilon \tag{30}$$

where

$$\begin{aligned}\mu[d(\varepsilon)]&=\mu\left\{\int_0^1 H[\varepsilon-\Delta(x)]dx\right\}=\int_0^1 \mu\{H[\varepsilon-\Delta(x)]\}dx\\&=\int_0^1\int_{-\infty}^{+\infty} H(\varepsilon-\Delta)f(\Delta)d\Delta dx\\&=\int_0^1\int_{-\infty}^{\varepsilon} f(\Delta)d\Delta dx=F(\varepsilon)\end{aligned} \tag{31}$$

According to Eq. (31) it is observed that the mean value function of the damage evolution is not other than the probability distribution function of the micro-fracture strain.

Performing the expectation operator to Eq. (29), we get

$$\mu(\overline{\sigma}^s)=\eta_s E\mu\left\{\int_0^1 \Delta(x)H[\varepsilon-\Delta(x)]dx\right\} \tag{32}$$

where

$$\begin{aligned}\mu\{\int_0^1 \Delta(x)H[\varepsilon-\Delta(x)]dx\}&=\int_0^1 \mu\{\Delta(x)H[\varepsilon-\Delta(x)]\}dx\\&=\int_0^1\int_{-\infty}^{+\infty}\Delta H(\varepsilon-\Delta)f(\Delta)d\Delta dx\\&=\int_0^1\int_{-\infty}^{\varepsilon}\Delta f(\Delta)d\Delta dx=G(\varepsilon)\end{aligned} \tag{33}$$

Then performing the expectation operator to Eq. (17) and considering Eqs. (30)–(33) we obtain

$$\begin{aligned}\mu(\overline{\sigma})&=\mu(\overline{\sigma}^d)+\mu(\overline{\sigma}^s)=[1-F(\varepsilon)]E\varepsilon+\eta_s EG(\varepsilon)\\&=\{1-\mu[d(\varepsilon)]\}E\varepsilon+\eta_s EG(\varepsilon)\end{aligned} \tag{34}$$

It is observed that Eq. (34) is the overall stress–strain relation under monotonic loading.

2.2.2. Unloading and reloading curve

Substituting Eq. (6) into Eq. (16), we obtain the unloading curve for the parallel system as follows:

$$\sigma_{\max}-\overline{\sigma}=\int_0^1 \phi_1(\varepsilon_{\max}-\varepsilon)dx+\int_0^1 \phi_2(\varepsilon_{\max}-\varepsilon)dx+\int_0^1 \phi_3(\varepsilon_{\max}-\varepsilon)dx \tag{35}$$

where

$$\begin{aligned}\int_0^1 \phi_1(\varepsilon_{\max}-\varepsilon)dx&=\int_0^1 H(\Delta-\varepsilon_{\max})E(\varepsilon_{\max}-\varepsilon)dx\\&=[1-d(\varepsilon_{\max})]E\varepsilon_{\max}-[1-d(\varepsilon_{\max})]\\E\varepsilon&=\overline{\sigma}^d_{\max}-\overline{\sigma}^d\end{aligned} \tag{36}$$

Hence we obtain the unloading expression for $\overline{\sigma}^d$ as follows:

$$\overline{\sigma}^d=[1-d(\varepsilon_{\max})]E\varepsilon \tag{37}$$

It is observed that the damage index remains constant during unloading. Then performing the expectation operator to Eq. (36), one obtains

$$\begin{aligned}\mu(\overline{\sigma}^d_{\max}-\overline{\sigma}^d)&=\{1-\mu[d(\varepsilon_{\max})]\}E(\varepsilon_{\max}-\varepsilon)\\&=[1-F(\varepsilon_{\max})]E(\varepsilon_{\max}-\varepsilon)\triangleq\Phi_1(\varepsilon_{\max}-\varepsilon)\end{aligned} \tag{38}$$

where $\triangleq$ denotes "define as".

Substitute Eq. (36) into Eq. (35), one obtains

$$\sigma^s_{\max}-\overline{\sigma}^s=\int_0^1 \phi_2(\varepsilon_{\max}-\varepsilon)dx+\int_0^1 \phi_3(\varepsilon_{\max}-\varepsilon)dx \tag{39}$$

Performing the expectation operator to Eq. (39), one gets

$$\begin{aligned}\mu(\sigma^s_{\max}-\overline{\sigma}^s)&=\mu\left[\int_0^1 \phi_2(\varepsilon_{\max}-\varepsilon)dx\right]+\mu\left[\int_0^1 \phi_3(\varepsilon_{\max}-\varepsilon)dx\right]\\&=\int_0^1 \mu[\phi_2(\varepsilon_{\max}-\varepsilon)]dx+\int_0^1 \mu[\phi_3(\varepsilon_{\max}-\varepsilon)]dx\end{aligned} \tag{40}$$

where

$$\begin{aligned}\mu[\phi_2(\varepsilon_{\max}-\varepsilon)]&=\mu\left\{H[\varepsilon_{\max}-\Delta(x)]H\left[\frac{\eta_s}{\eta_e}\Delta-(\varepsilon_{\max}-\varepsilon)\right]\eta_e E(\varepsilon_{\max}-\varepsilon)\right\}\\&=\eta_e E(\varepsilon_{\max}-\varepsilon)\int_{-\infty}^{+\infty} H[\varepsilon_{\max}-\Delta]H\left[\frac{2\eta_s}{\eta_e}\Delta-(\varepsilon_{\max}-\varepsilon)\right]f(\Delta)d\Delta\\&=\eta_e E(\varepsilon_{\max}-\varepsilon)\int_{(\eta_e/2\eta_s)(\varepsilon_{\max}-\varepsilon)}^{\varepsilon_{\max}} f(\Delta)d\Delta\\&=\eta_e E(\varepsilon_{\max}-\varepsilon)\left\{F(\varepsilon_{\max})-F\left[\frac{\eta_e}{2\eta_s}(\varepsilon_{\max}-\varepsilon)\right]\right\}\\&=\eta_e E(\varepsilon_{\max}-\varepsilon)\left\{\mu[d(\varepsilon_{\max})]-F\left[\frac{\eta_e}{2\eta_s}(\varepsilon_{\max}-\varepsilon)\right]\right\}\end{aligned} \tag{41}$$

$$\begin{aligned}\mu[\phi_3(\varepsilon_{\max}-\varepsilon)]&=\mu\left[H(\varepsilon_{\max}-\Delta)H\left[(\varepsilon_{\max}-\varepsilon)-\frac{2\eta_s}{\eta_e}\Delta\right]2\eta_s E\Delta\right]\\&=2\eta_s E\int_{-\infty}^{+\infty}\Delta H(\varepsilon_{\max}-\Delta)H\left[(\varepsilon_{\max}-\varepsilon)\quad-\frac{2\eta_s}{\eta_e}\Delta\right]f(\Delta)d\Delta\\&=2\eta_s E\int_{-\infty}^{(\eta_e/2\eta_s)(\varepsilon_{\max}-\varepsilon)}\Delta f(\Delta)d\Delta=2\eta_s EG\left[\frac{\eta_e}{2\eta_s}(\varepsilon_{\max}-\varepsilon)\right]\end{aligned} \tag{42}$$

Then we define

$$\begin{aligned}\Phi_2(\varepsilon_{\max}-\varepsilon)&=\mu\left[\int_0^1 \phi_2(\varepsilon_{\max}-\varepsilon)dx\right]=\eta_e E(\varepsilon_{\max}\quad-\varepsilon)\\&\times\left\{F(\varepsilon_{\max})-F\left[\frac{\eta_e}{2\eta_s}(\varepsilon_{\max}-\varepsilon)\right]\right\}\end{aligned} \tag{43}$$

$$\Phi_3(\varepsilon_{\max}-\varepsilon)=\mu\left[\int_0^1 \phi_3(\varepsilon_{\max}-\varepsilon)dx\right]=2\eta_s EG\left[\frac{\eta_e}{2\eta_s}(\varepsilon_{\max}-\varepsilon)\right] \tag{44}$$

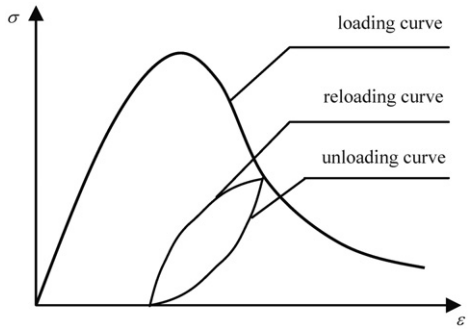

Fig. 8. Mean value stress–strain curve.

Performing the expectation operator to Eq. (35) and considering Eqs. (36)–(44), we obtain

$$\begin{aligned}\mu(\overline{\sigma}_{\max}-\overline{\sigma}) &= \mu(\overline{\sigma}^{d}_{\max}-\overline{\sigma}^{d}+\overline{\sigma}^{s}_{\max}-\overline{\sigma}^{s})\\ &= \mu(\overline{\sigma}^{d}_{\max}-\overline{\sigma}^{d})+\mu(\overline{\sigma}^{s}_{\max}-\overline{\sigma}^{s}) = \Phi_1(\varepsilon_{\max}-\varepsilon)\\ &\quad +\Phi_2(\varepsilon_{\max}-\varepsilon)+\Phi_3(\varepsilon_{\max}-\varepsilon)\end{aligned} \tag{45}$$

Eq. (45) could be expressed using the following abstract function:

$$\mu(\overline{\sigma}_{\max}-\overline{\sigma}) = \mathcal{H}(\varepsilon_{\max}-\varepsilon) \tag{46}$$

where

$$\mathcal{H}(x) \triangleq \Phi_1(x)+\Phi_2(x)+\Phi_3(x) \tag{47}$$

Performing the similar procedure to Eq. (10), we obtain the mean value expression for the reloading curve as follows:

$$\mu(\overline{\sigma}-\overline{\sigma}_{\min}) = \mathcal{H}(\varepsilon-\varepsilon_{\min}) \tag{48}$$

Noting that if the current strain ε exceeds the original unloading strain $\varepsilon_{\max}$, the mean value stress–strain path will return to the monotonic curve expressed by Eq. (34). The mean value stress–strain curve is illustrated in Fig. 8.

2.2.3. Hysteretic loop

It is observed from Fig. 8 that the local hysteretic loop, which is an essential non-linear characteristic of the quasi-brittle material, is made up of the unloading and the reloading curves expressed by Eqs. (46) and (48), respectively. However, under the complicated repeated loading such as the earthquake, a suite of hysteretic rules is required to describe the sequential hysteretic loops before returning to the initial monotonic loading curve. In the present paper, the quasi-brittle material subjected to the local hysteretic loading is modeled as the parallel element bundle shown in Fig. 7. The uncracked elements remain elastic during the local hysteretic loading, and the elastic-perfectly plastic behaviors are observed for the cracked elements according to the former discussions. Since all the elements are attached to the rigid bar on the end, the strain within the bundle is uniformly distributed for all the elements. On the other hand, this overall strain for each cracked element is equal to the strain summation of the elastic spring and the sliding element. And the strain distribution between the elastic element and the sliding element is influenced by the loading history. Hence not only the current strain but also the strain history is required to determine the hysteretic responses of the model under non-uniform repeated loading.

The direct numerical implementation for this model is difficult and time consuming because the internal behaviors of each element should be tracked during the analysis. By noting Iwan [14] and Jayakumar [15], it is demonstrated that the hysteretic behavior of the parallel buddle could be exactly described through several phenomenological rules. Therefore, based on the loading, unloading and reloading equations developed in the former chapter, two rules for the parallel element model under repeated loading are proposed as follows (see Fig. 9):

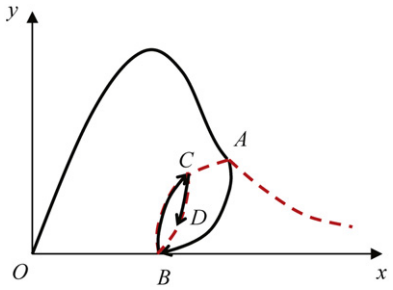

Fig. 9. Local hysteretic response of quasi-brittle materials.

Rule 1 *(Incomplete loops)*: The equation of any hysteretic response curve can be obtained by the following expressions:

$$\begin{cases}\sigma = [1-F(\varepsilon)]E\varepsilon+\eta_s EG(\varepsilon) & \text{loading curve}\\ \sigma^*-\sigma = \mathcal{H}(\varepsilon^*-\varepsilon) & \text{unloading curve}\\ \sigma-\sigma^* = \mathcal{H}(\varepsilon-\varepsilon^*) & \text{reloading curve}\end{cases} \tag{49}$$

where (ε^*,σ^*) is the load reversing point for that branch, function $\mathcal{H}(\bullet)$ was defined in Eq. (47).

Rule 2 *(Completed loops)*: If an interior curve under continues loading or unloading crosses a curve described in a previous load cycle, the force–deformation curve follows that of the previous cycle.

3. Model verification

3.1. Random distribution for threshold strain random field

As mentioned before, the fracture strain $\Delta(x)$ is modeled as a stationary random field with the mean value μ_Δ and the standard deviation V_Δ. It is clear that the first-order density functions should be specified before the stress–strain curve is calculated. The lognormal distribution is usually adopted to describe the randomness of the fracture strength for concrete [29]. In the micro-level, the fracture stress is proportional to the fracture strain. Thus it is reasonable to choose lognormal distribution to describe the rupture strain field. The lognormal density distribution function could be expressed as

$$f(\Delta) = \frac{1}{\sqrt{2\pi}\Delta\zeta}\exp\left\{-\frac{1}{2}\left[\frac{\ln(\Delta)-\lambda}{\zeta}\right]^2\right\} \tag{50}$$

where the parameters λ and ζ are:

$$\lambda = E\left[\ln\Delta(x)\right] = \ln\left(\frac{\mu_\Delta}{\sqrt{1+V_\Delta^2/\mu_\Delta^2}}\right) \tag{51}$$

$$\zeta^2 = \mathrm{var}[\ln\Delta(x)] = \ln(1+V_\Delta^2/\mu_\Delta^2) \tag{52}$$

Then $Z(x) = \ln\Delta(x)$ is a homogeneous normal random field with the mean value λ and the standard deviation ζ.

On the other side, the shape of the Weibull distribution is similar with the lognormal distribution, but it is easier to compute the cumulative distribution for the Weibull distribution by using its analytical solution. Thus we adopt Weibull distribution as one of the possible simplification for our model. The two-parameter

Weibull density distribution function is

$$f(\Delta)=\frac{b}{a}\left(\frac{\Delta}{a}\right)^{b-1}\exp\left[-\left(\frac{\Delta}{a}\right)^{b}\right] \tag{53}$$

And the corresponding cumulative distribution function is

$$F(\Delta)=1-\exp\left[-\left(\frac{\Delta}{a}\right)^{b}\right] \tag{54}$$

The mean value of the Weibull distribution with parameters a and b is

$$\mu_{\Delta}=a\Gamma\left(1+\frac{1}{b}\right) \tag{55}$$

and the variance is

$$V_{\Delta}^{2}=a^{2}\left[\Gamma\left(1+\frac{2}{b}\right)-\Gamma^{2}\left(1+\frac{1}{b}\right)\right] \tag{56}$$

where $\Gamma(x)$ is the Gamma function.

3.2. Numerical simulation

To verify the foregoing analytical expressions derived the parallel element model, numerical results based on both the analytical solutions and the stochastic simulations are calculated and compared in this section. Both the lognormal distribution and the Weibull distribution are adopted for the simulation. The

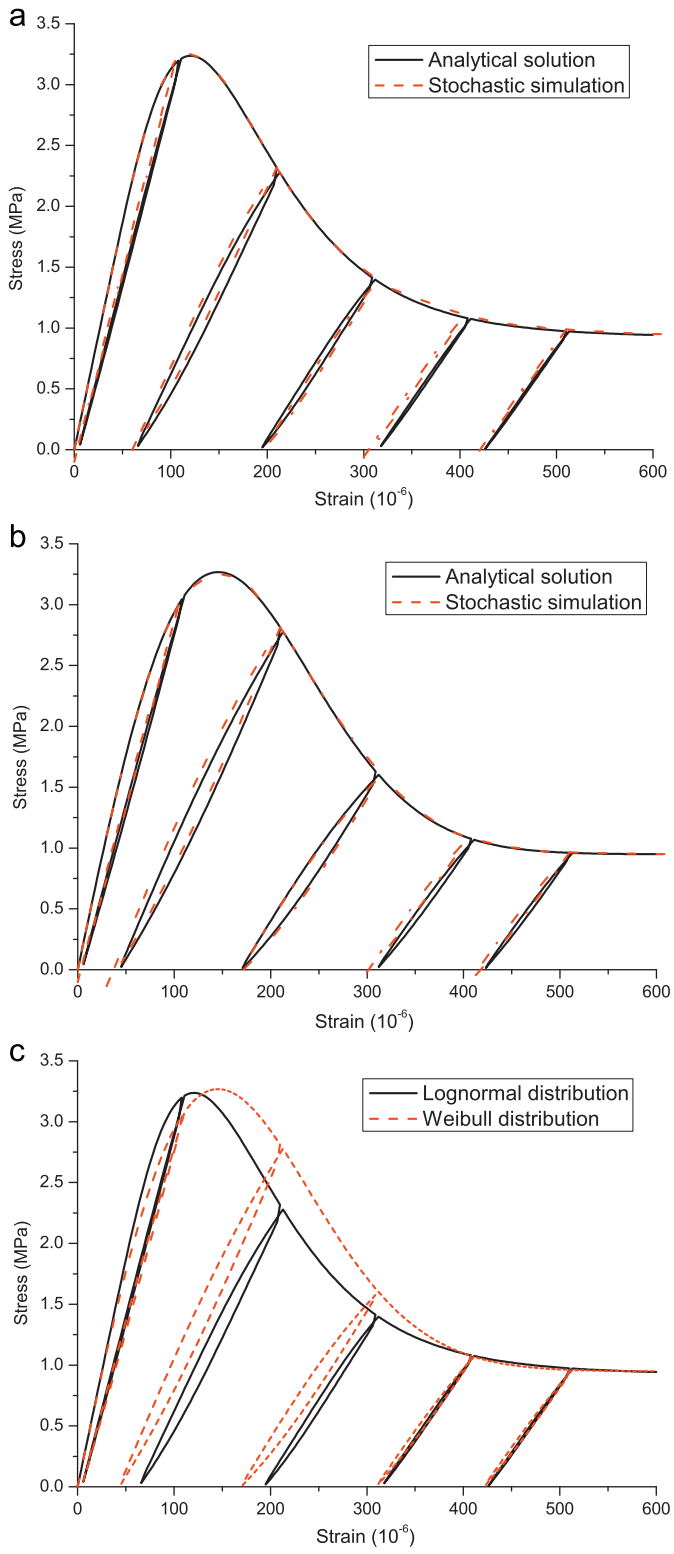

Fig. 10. Comparison between numerical stress–strain curves: (a) analytical solution vs. random simulation (lognormal distribution), (b) analytical solution vs. random simulation (Weibull distribution), and (c) lognormal distribution vs. Weibull distribution.

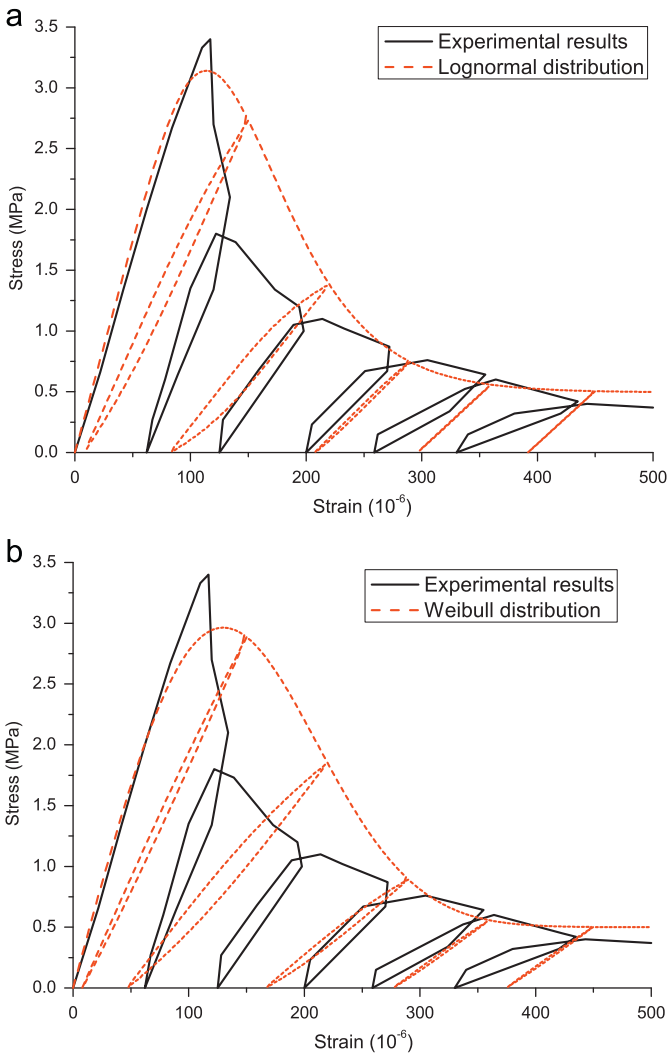

Fig. 11. Repeated tensile loading curves: (a) stress–strain response of lognormal random field and (b) stress–strain response of Weibull random field.

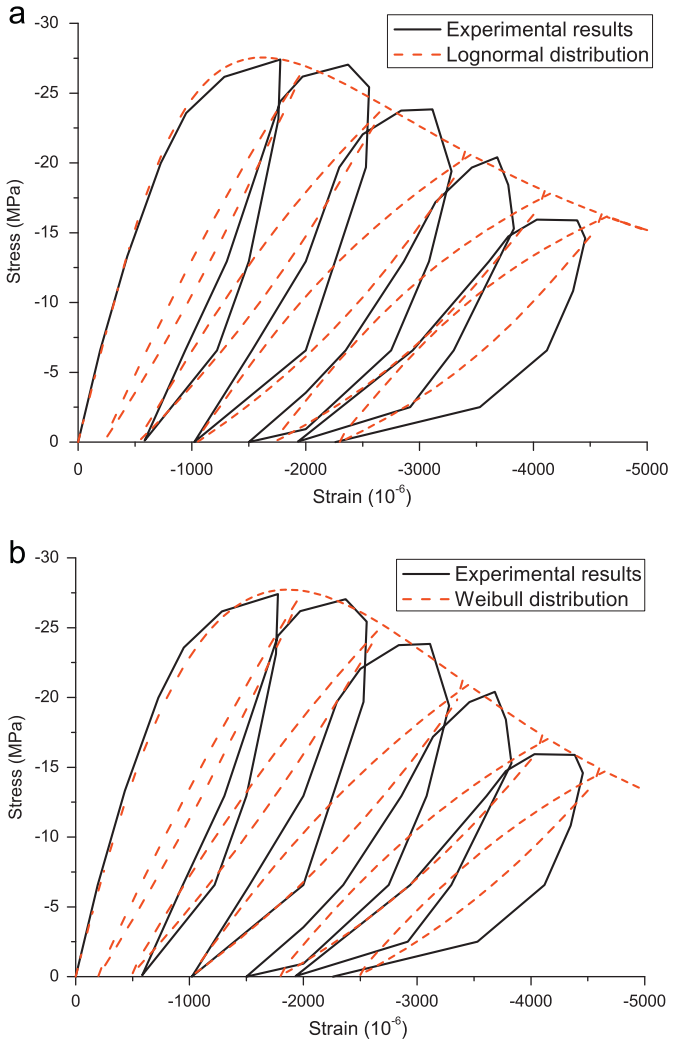

Fig. 12. Repeated compressive loading curves: (a) stress–strain response of lognormal random field and (b) stress–strain response of Weibull random field.

numerical results are illustrated in Fig. 10 (E=37,559 MPa, η_s=0.15, η_e=0.3, λ=5.0, ζ=0.45, a=190 and b=2.0)

It is observed that the analytical stress–strain curves agree well with the stochastic simulated curves in Fig. 10. However, the stochastic simulation method is expensive because the loading path of each element should be tracked. It is indicated that both the lognormal and the Weibull random fields can reproduce the complicated hysteretic deteriorating behaviors for the quasi-brittle materials. But the difference between them is of particularly interesting. The increasing part of the stress–strain curve of the lognormal random field is higher due to the initial horizontal part of the density function.

3.3. Results for concrete

Taylor [30] conducted the repeated tensile loading tests for concrete and obtained the stress–strain curves illustrated in Fig. 11 against the analytical curves simulated with the proposed model. The elastic modulus of the concrete specimen is E=34,810 MPa. The parameters of the lognormal type model are found to be λ=5.0, ζ=0.35, η_s=0.09 and η_e=0.25. And the parameters of the Weibull type model are a=180, b=2.4, η_s=0.09 and η_e=0.20.

The testing results of the repeated compressive experiment conducted by Karson and Jirsa [31] are plotted in Fig. 12 against the numerical predictions. The elastic modulus is identified to be E=32,000 MPa. The parameters of the lognormal type model are λ=7.38, ζ=0.71, η_s=0.12 and η_e=0.25. And the parameters of the Weibull type model are a=2100, b=1.35, η_s=0.13 and η_e=0.25.

It is observed that the stress–strain responses generated from the lognormal distribution are in better agreement with the experimental data than those from the Weibull distribution. On the other hand, the numerical implementation of the Weibull distribution is more efficient. Hence the selection of the distribution should be considered based on the balance between the accuracy and the efficiency.

4. Summary and conclusions

A micromechanical model has been developed in this paper for the quasi-brittle materials subjected to hysteretic loading. Based on the theoretical derivation and the numerical simulation, several conclusions can be drawn:

- The hysteretic deteriorating model proposed in this paper is able to represent the softening and the hysteretic behaviors for the quasi-brittle materials under non-uniform repeated loading.
- Not only the current state variables but also the loading histories are considered within this model.
- The stochastic averaging procedure is a simple but efficient way to bridge the response between the micro-scale and the macro-scale.
- Combining with the appropriate method for the structure analysis, this model could represent the subtle dynamic responses for structures.

Acknowledgement

Financial supports from the National Science Foundation of China for key project (Grant no. 90715033) are greatly appreciated.

References

[1] J.W. Ju, On energy-based coupled elastoplastic damage theories—constitutive modeling and computational aspects, Int. J. Solid Struct. 25 (7) (1989) 803–833.
[2] R. Faria, J. Oliver, M. Cervera, A strain-based plastic viscous-damage model for massive concrete structures, Int. J. Solid Struct. 34 (14) (1998) 1533–1558.
[3] J.Y. Wu, J. Li, R. Faria, An energy release rate-based plastic-damage model for concrete, Int. J. Solid Struct. 43 (3–4) (2006) 583–612.
[4] F. Preisach, On magnetic aftereffect, Z. Phys. 94 (1935) 277–302.
[5] M.A. Krasnoselskii, Systems with Hysteresis, Nauka, Moscow, 1983.
[6] I.D. Mayergoyz, Mathematical models of hysteresis, Phys. Rev. Lett. 56 (1986) 1518–1521.
[7] P. Ge, M. Jouaneh, Generalized preisach model for hysteresis nonlinearity of piezoceramic actuators, Precision Eng. 20 (2) (1997) 99–111.
[8] D. Hughes, J.T. Wen, Preisach modeling of piezoceramic and shape memory alloy hysteresis, Smart Mater. Struct. 6 (1997) 287–300.
[9] F.T. Peirce, Tensile test for cotton Yarns—the weakest link, J. Texture Inst. 17 (1926) 355–370.
[10] H.E. Daniels, The statistic theory of the strength of bundles of threads, I. Proc. Roy. Society 183 (1945) 405–435.
[11] S. Kandarpa, D.J. Kirkner, Stochastic damage model for brittle materiel subjected to monotonic loading, J. Eng. Mech. ASCE 126 (8) (1996) 788–795.
[12] A. Rinaldi, D. Krajcinovic, S. Mastilovic, Statistical damage mechanics—constitutive relations, J. Theor. Appl. Mech 44 (3) (2006) 585–602.
[13] A. Rinaldi, D. Krajcinovic, S. Mastilovic, Statistical damage mechanics and extreme value theory, Int. J Damage Mech. 16 (1) (2007) 57–76.
[14] W.D. Iwan, A distributed-element model for hysteresis and its steady-state dynamic response, J. Appl. Mech 33 (1966) 893–900.
[15] P. Jayakumar, Modeling and identification in structural dynamics. Ph.D. Thesis, California Institute of Technology, Pasadena, California, 1987.
[16] D.Y. Chiang, The generalized Masing models for deteriorating hysteresis and cyclic plasticity, Appl. Math. Model 23 (11) (1999) 847–863.
[17] D.Y. Chiang, K.H. Su, C.H. Liao, A study on subsequent yield surface based on the distributed-element model, Int. J. Plasticity 18 (1) (2002) 51–70.
[18] D.J. Segalman, M.J. Starr, Inversion of Masing models via continuous Iwan systems, Int. J. Nonlin. Mech. 43 (1) (2007) 74–80.

[19] J. Eibl, B. Schmidt-Hurtienne, Strain-rate-sensitive constitutive law for concrete, J. Eng. Mech. ASCE 125 (12) (1996) 1411–1420.
[20] H.R. Valipour, L. Huynh, S.J. Foster, Analysis of RC beams subjected to shock loading using a modified fibre element formulation, Comput. Concrete Res. 6 (5) (2009) 377–390.
[21] Z.P. Bazant, S.D. Pang, Activation energy based extreme value statistics and size effect in brittle and quasi-brittle fracture, J. Mech. Phys. Solids 55 (1) (2007) 91–131.
[22] J. Li, Q.Y. Zhang, Study of stochastic damage constitutive relationship for concrete material, J. Tongji University 29 (10) (2001) 1135–1141 (in Chinese).
[23] G. Masing, Eigenspannungen und verfestigung beim messing self stretching and hardening for brass, in: Proceedings of the Second International Congress for Applied Mechanics, Zurich, Switzerland, 1926, pp. 332–335.
[24] W.D. Iwan, A.O. Cifuentes, A model for system identification of degrading structures, Earthq. Eng. Struct. Dyn. 14 (6) (1986) 877–890.
[25] S.A. Ashrafi, W.S. Andrew, Generalized Masing approach to modeling hysteretic deteriorating behavior, J. Eng. Mech. ASCE 133 (5) (2007) 495–505.
[26] S.A. Ashrafi, A.W. Smyth, Adaptive parametric identification scheme for a class of nondeteriorating and deteriorating nonlinear hysteretic behavior, J. Eng. Mech. 134 (6) (2008) 482–494.
[27] J.H. Ye, On stress–strain curve and residual strength of rock, Yantu Gongcheng Xuebao 12 (2) (1990) 100–102 (in Chinese).
[28] J.N. Tao, On stability analysis of rock, Yantu Gongcheng Xuebao 12 (2) (1990) 102–106 (in Chinese).
[29] Z.P. Bazant, E. Becq-Giraudon, Statistical prediction of fracture parameters of concrete and implications for choice of testing standard, Cement Concrete Res. 32 (4) (2002) 529–556.
[30] R.L. Taylor, FEAP: a finite element analysis program for engineering workstation. Report No. UCB/SEMM-92 (Draft Version), Department of Civil Engineering, University of California, Berkeley, California, 1992.
[31] I.D. Karson, J.O. Jirsa, Behaviour of concrete under compressive loadings, J. Struct. Div. ASCE 95 (12) (1969) 2535–2563.
[32] S. Kandarpa, D.J. Kirkner, B.F. Spencer, Stochastic damage model for brittle materiel subjected to monotonic loading, J. Eng. Mech. ASCE 122 (8) (1996) 788–795.